

# TANTALUS I: A DEDICATED STORAGE RING SYNCHROTRON RADIATION SOURCE†

E. M. ROWE

*Physical Sciences Laboratory, University of Wisconsin, Stoughton, Wisconsin, USA*

and

F. E. MILLS

*Brookhaven National Laboratory, Upton, New York, USA*

A small electron storage ring has been operated at the Physical Sciences Laboratory of the University of Wisconsin as a synchrotron radiation source for the investigation of the optical and electronic properties of solids, liquids and gases in the vacuum ultraviolet and soft X-ray region of the electromagnetic spectrum. The storage ring has proven to be a nearly ideal source for these investigations. The storage ring has also been shown to have fundamental advantages over electron synchrotrons more commonly used for this work. These advantages are stability of the electron beam as a source of photons in position, size and intensity, low levels of high energy particle radiation in the vicinity of the machine and operating vacua consistent with the requirements of the experimental program. A description of the constructional details of the storage ring, a report of its operating characteristics and a discussion of the research program that it serves is given. A summary of projects now being carried out to increase the utility of the storage ring is included.

## 1. INTRODUCTION

Parker pointed out in a recent article in *Particle Accelerators*<sup>1</sup> that there is still much interesting and even exciting physics to be done with low energy accelerators. In addition, he pointed out many interesting applications of such machines, which if not pure science, are at least very useful. We would like to describe an electron machine that operates in an energy range long since abandoned by those working in photon and electron interaction physics as having yielded its exciting discoveries, but which is now being exploited by that 'legion of patient spectroscopists' that Professor Weisskopf<sup>2</sup> spoke about with such affection at the 1971 International Conference on High Energy Accelerators, to explore a hitherto inaccessible portion of the electromagnetic spectrum.

This machine, a 240-MeV electron storage ring, has an interesting distinction: its success as a research instrument is solely the result of the useful application of a normally unwanted by-product of its operation. This is, of course, synchrotron radiation, long looked upon by the accelerator

builder as yet another manifestation of the essential perversity of nature: the very process which is involved in almost every experiment performed with high energy electron machines, bremsstrahlung radiation, also limits our ability to raise the energy of such machines indefinitely.

However, after the prediction,<sup>3</sup> observation,<sup>4,5</sup> and theoretical treatment<sup>6</sup> of synchrotron radiation, Fano, and others, pointed out that the unique properties of this phenomenon could be of great aid in the study of the electronic and optical properties of solids, liquids and gases. The application of modern optical techniques to investigations in the ultraviolet beyond the LiF cutoff at 1050 Å is difficult because of the lack of continuum sources of adequate intensity. This is particularly true of the 50 to 500 Å range. In addition, this portion of the spectrum is a region of strong absorption, thus this range is also called the vacuum ultraviolet. Utilization of such sources as do exist is made difficult by the fact that most of them are relatively high pressure gaseous discharge devices. Therefore, it was reasonable that synchrotron radiation, by virtue of its continuum nature and easily calculable spectral distribution represented an attractive possibility for exploring the vacuum ultraviolet.

† This work was performed under the auspices of the U.S. Atomic Energy Commission, the Air Force Office of Scientific Research, and the Advanced Research Projects Agency.

There was, in addition, the fact that the electron machines that produce it operate at reasonable pressures, thus solving or at least easing the vacuum separation problems.

Subsequently, pioneering work by Tomboulion and Hartman,<sup>7</sup> and by Maden and Codling<sup>8</sup> verified the predictions. As a result, over the past ten years, vigorous programs to study the interaction of electromagnetic radiation with matter in this region of the spectrum, first in atomic physics then in solid state physics and more recently in chemistry and biology have been instituted at electron synchrotrons at the NBS, Tokyo, Frascati, Hamburg, and Daresbury.

Six years ago, when the machine to be described was being prepared as an instrument to study the physics of particle accelerators, Professor P. G. Kruger of the University of Illinois pointed out its existence to other members of a subcommittee of the Solid State Panel of the American Academy of Sciences then sitting to consider the uses of synchrotron radiation in solid state physics.<sup>9</sup> This, in turn, led to contact being established between the authors and Professor F. C. Brown, also of the University of Illinois and a member of the sub-

committee. From this contact came the beginnings of the synchrotron radiation research program at the Center, then part of the MURA Laboratory, now part of the Physical Sciences Laboratory of the University of Wisconsin. Since these beginnings, the research program at the Center has grown from one imaginative and foresighted investigator to the present at which time there are fourteen groups actively pursuing researches at the ring and nine more groups preparing experiments to be conducted at the ring. In this time of tight research budgets and even tighter travel budgets it is perhaps indicative of the excitement now pervading the field of vacuum ultraviolet physics in the United States because of the availability of a totally dedicated synchrotron radiation source that the majority of users come from outside the State of Wisconsin, some from as far away as the University of Southern California and the IBM Research Laboratories in New York.

## 2. MAGNET SYSTEM

The Storage Ring is shown in Fig. 1 and a plan view is given in Fig. 2. A table listing its major

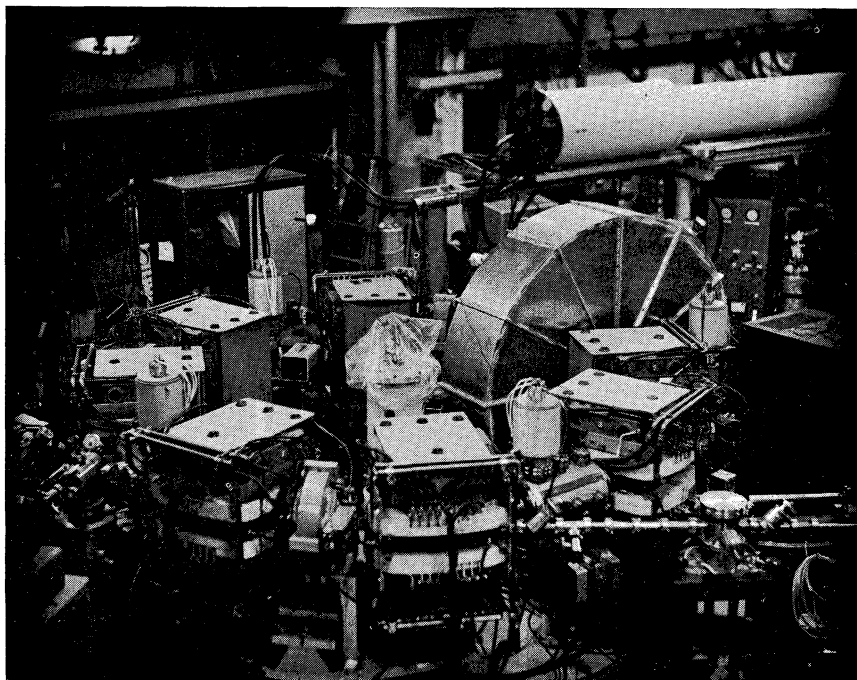


FIG. 1. Storage ring. Photon beam lines and separation chambers appear at lower right and left. Cylindrical object at top is the inflector spark gap energy storage line enclosure.

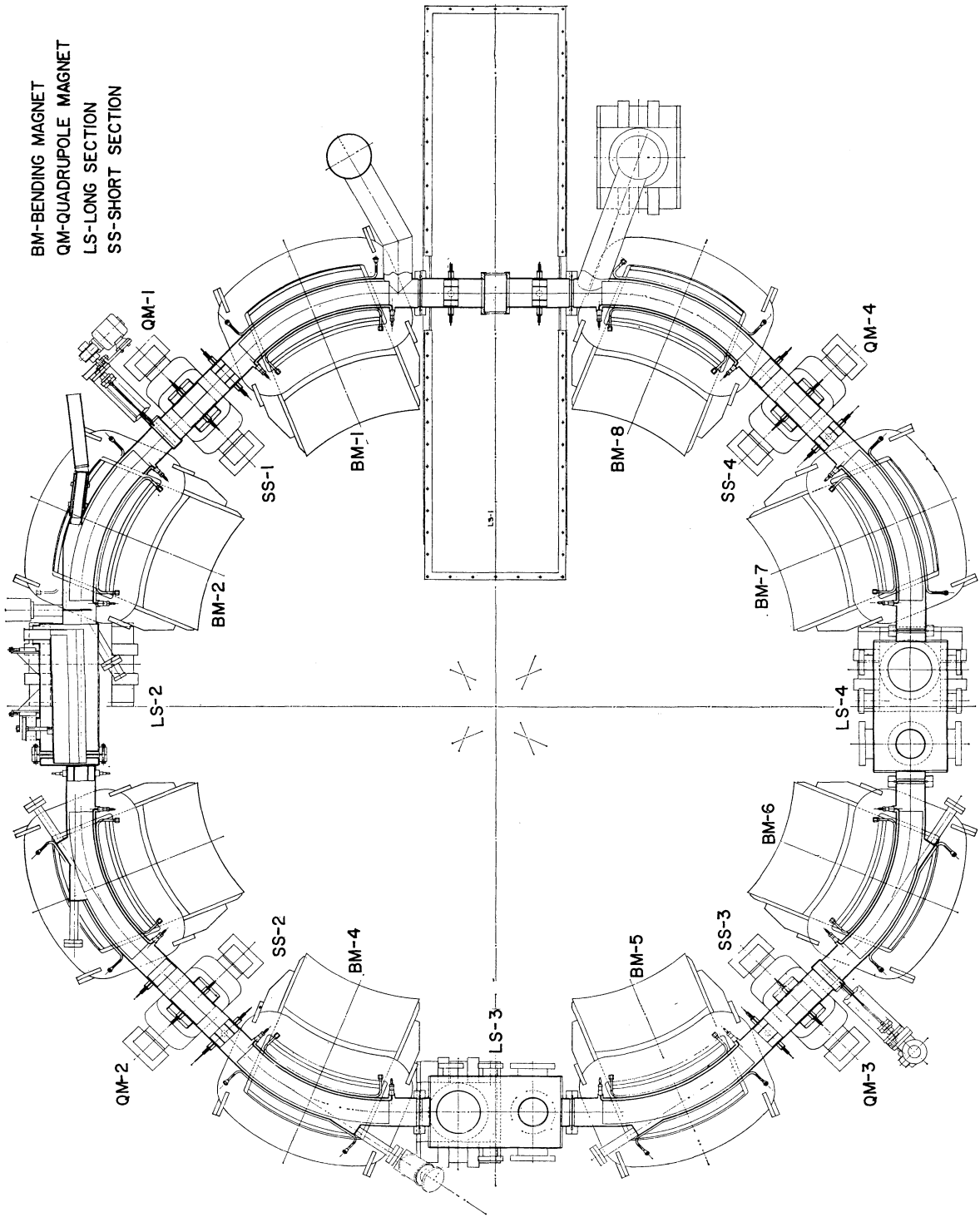


FIG. 2. Storage ring plan view. Injection straight section is at top, radiofrequency accelerating cavity is at right.

TABLE I  
Parameters for 240-MeV Storage Ring

<i>Magnet</i>	
Focusing Type	AG, Separated Function
Focusing Order	0/2, D, O, D, f, D, O, D, 0/2
Field Index in Bending Magnets	Variable, $-0.34 \leq n \leq 0.34$
Field Gradient in Quadrupoles	Variable, 1.6 kG cm <sup>-1</sup> max
Field at Injection	2.36 kG
Field at Maximum Energy	12.3 kG
Bending Radius	0.635 m
Average Radius	1.50 m
Tune	Variable, $1.0 < \nu_x, \nu_y < 1.5$
<i>Injection system</i>	
Type	50-MeV FFAG Electron Synchrotron
Injection Energy $e^-$	45 MeV
Injection Current $e^-$ (per pulse)	50 mA
Injection Energy Spread	$\pm 125$ kV
Inflector	Delay Line, No Septum
<i>RF system</i>	
Frequency	Tunable, 31.9 MHz nominal
Harmonic Number	1
Number of Cavities	1
Maximum Volts per Turn	20 kV
Maximum Power Available to Cavity and Beam	20 kW

parameters is given in Table I. It will be noticed that the magnet back legs are on the inside of the machine. This design was chosen originally for easy access to the vacuum chamber, a feature useful in a machine designed as an instrument to study electron-positron storage rings. As the vacuum ultraviolet research program developed this feature was to become of vital importance since it allowed the easy installation of synchrotron radiation beam ports.

The design of the storage ring is unconventional in that it has neither a combined function nor a separated function guide magnet. Radial focusing is provided by quadrupoles while vertical focusing is provided by the large (22.5°) edge angles of the bending magnets. The bending magnets have, nominally, no gradient. However, through the use of coils mounted on the magnet poles, quadrupole and sextupole components may be superimposed on the dipole field. There are no provisions for dipole corrections. The uniformity of the bending magnets and the alignment precision plus the fact that the disposition of the magnets was determined by use of a computer to minimize the first six harmonics of the field errors rendered such corrections unnecessary. The median plane of all the

magnets was determined<sup>10</sup> with considerable accuracy, thus provision for vertical steering in the ring was not necessary either.

The magnets and quadrupoles are laminated of 0.060 in. 1010 steel to reduce eddy currents during acceleration to 240 MeV after injection. It should be remarked here that lamination also decreases the settling time of a large magnet after a change of excitation. This is not so important for a machine that operates for long periods at fixed field, such as a cyclotron, but in a machine like the one under discussion that must accelerate after injection, long settling times can be troublesome.

The dipoles and quadrupoles are run in series from a common power supply consisting of a pair of 250 V, 400 A amplidynes connected in series, driven by a 150 horsepower high slip motor. These generators are characterized by extremely large (60 dB) power gain, and in fact account for most of the gain in the magnet field servo loop. The magnet field supply<sup>11</sup> exhibits good stability, better than one part in 10<sup>4</sup> long term, and remarkable frequency response: it will, for example, produce full output current into a resistive load at frequencies up to 40 cps. The response of the power supply to a 3 cps triangular drive signal is

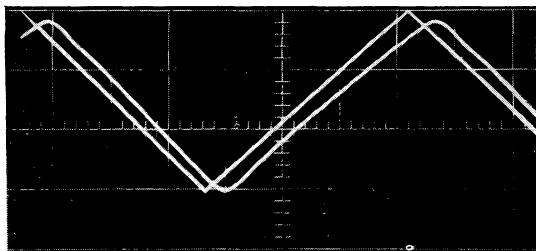


FIG. 3. Magnet power supply input and output signals. Output current is shown on trace displaced slightly to the right. Repetition rate is 3 Hz and vertical calibration is 50 A/cm.

shown in Fig. 3. In this case, the load was the storage ring magnet.

### 3. INJECTION SYSTEM

The injector for the storage ring is a 50-MeV FFAG electron synchrotron.<sup>12</sup> The bunched beam is extracted from this machine<sup>13</sup> in a single turn, and transported 50 ft to the storage ring.

Upon arrival at the ring, the beam passes through two magnetic elements. The first of these is a pulsed, water-cooled, air-cored dipole producing a peak field of 0.7 T, utilizing a cosine theta winding mounted in the fringe field of BM-2. This magnet bends the beam out, away from BM-2. After emerging from this element, the beam, still traveling in the fringe field of BM-2, is bent back towards the machine and enters the inflector which has no septum. The inflector bends the beam onto the injection orbit which is approximately 2 cm displaced radially from the central orbit. Since there is no pulsed bump in the ring, injection is nominally at zero betatron amplitude and the inflector must be off by the time the injected beam completes the first revolution. The inflector pulse is generated by an energy storage line and spark gap system which is shown diagrammatically in Fig. 4. The characteristic impedance of the system is  $25\Omega$  and the pulse voltage is 65 kV. The rise and decay time of the pulse is 4 nsec. Figure 5 shows the beam path through the injection system.

After injection and capture, the radiofrequency accelerating system is used to move the beam to the central orbit. The reasons for injecting on an off-center orbit are of historical interest only and will not be discussed here.

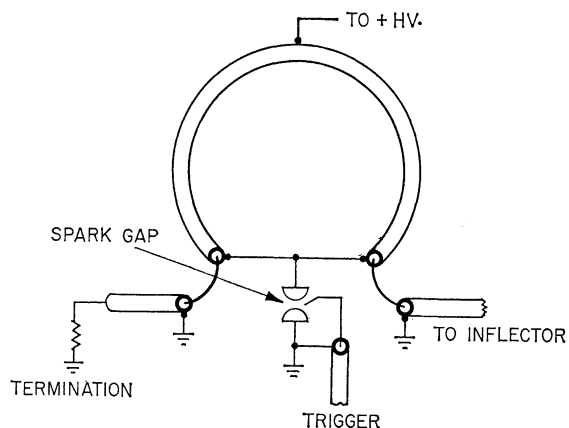


FIG. 4. Inflector spark gap circuit. All reflections from inflector are absorbed in the termination.

### 4. THE RF SYSTEM

At 240 MeV, an electron in the storage ring loses 470 eV per turn to synchrotron radiation. However, in order to assure adequate beam lifetime against quantum fluctuations, inelastic scattering off of the orbital electrons of residual gas molecules, bremsstrahlung and Touschek effect, accelerating voltages considerably larger than might be expected are required. In fact, the accelerating system on the storage ring operates normally at 10 keV peak per turn. It can produce 20 keV peak per turn.

Since the beam injection orbit is displaced from the central orbit, the radiofrequency system must have some frequency agility and the accelerating cavity must, of course, be tunable. The cavity tuning system used on the storage ring has some interesting aspects. In order that large accelerating potentials may be developed without the expenditure of similarly large amounts of power, the accelerating cavity must have a reasonably high  $Q$ . On the other hand, the tuning system must be able to change the resonant frequency of the cavity by several hundreds of kilohertz in a fraction of a second. While an electromechanical tuning system such as those perfected by Schnell<sup>14</sup> might have been developed, a different approach, utilizing ferrites has been taken. Usually, the introduction of ferrites into a radiofrequency cavity reduces the  $Q$  of the cavity by orders of magnitude. This, however, occurs because normally most of the energy in the cavity is stored in the ferrite. In this case, since the required frequency shift is less than 2 MHz out of

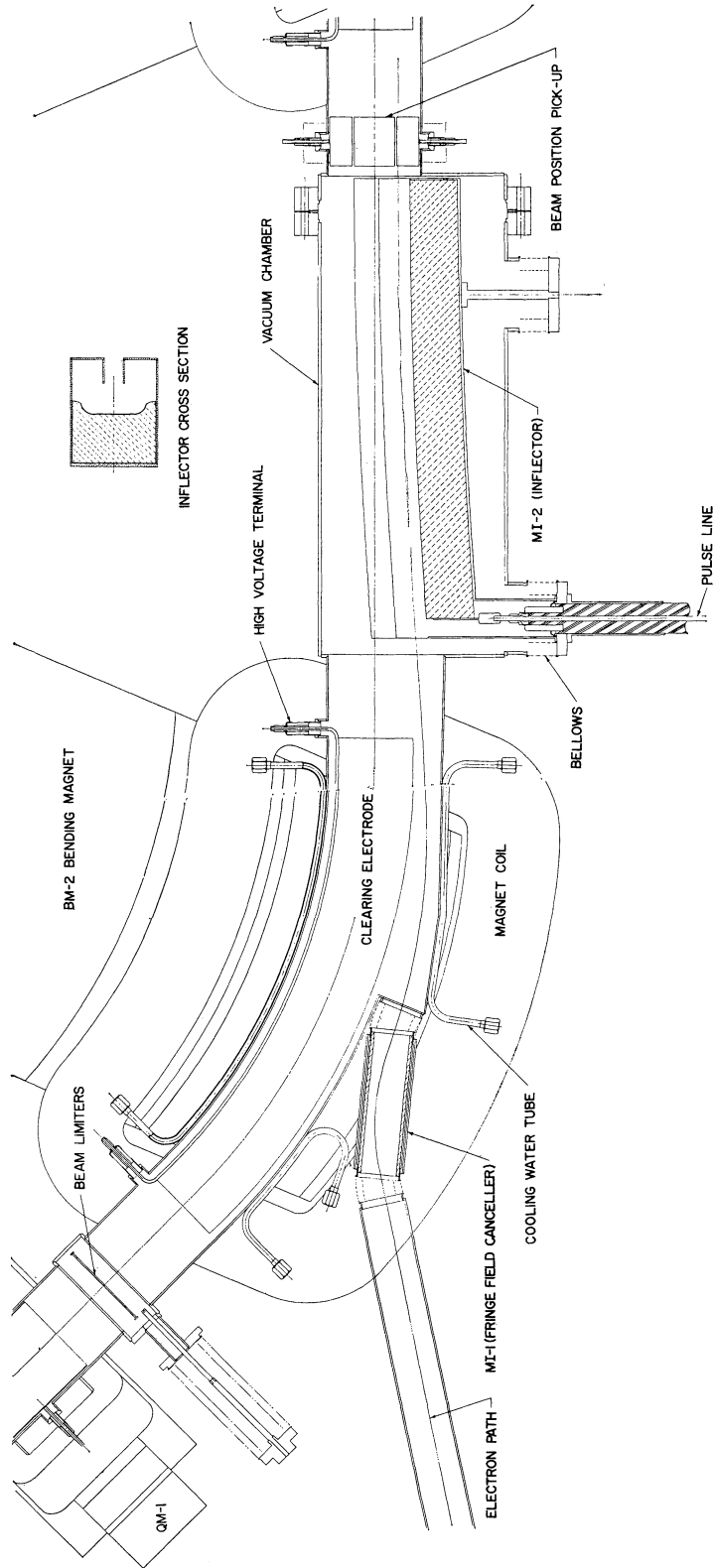


FIG. 5. Beam path through the injection system.

32 MHz, only a small part of the total stored energy in the cavity need be stored in the tuning system. In the cavity tuning system developed for the storage ring, this was accomplished by coupling the ferrite tuning structure to the cavity very loosely. The ferrite rings, interleaved with aluminum disks of larger diameter, are mounted on 2 cm diameter copper pipes that pass completely through the cavity. The aluminum plates between the rings serve both to transfer heat from the ferrite rings to the copper pipes through which water is passed, and also to shield the rings from the high electric fields in the cavity. The copper pipes also carry the bias current which causes the variation in the incremental permeability of the ferrite that tunes

the cavity. There are three such assemblies in the cavity using a total of 60, 10 cm diameter, 1.25 cm thick rings. The ferrite is Ferroxcube 4-C.

In operation, when the bias current is low, the incremental permeability of the ferrite is high. This results in the inductances of the copper pipes being high and the cavity being resonant at very nearly its natural frequency. As the bias current is raised, the incremental permeability of the ferrite decreases and the copper pipes become more like short circuits across the cavity. As a result, the cavity resonant frequency increases.

Changing the bias current from an initial value of 100 A to a final value of 900 A tunes the cavity from 31.4 MHz to 32.8 MHz. In this range of magnetization, 10 to 100 ampere turns per centimeter, the ferrite loss is low and the cavity  $Q$  is in excess of 2500 over the frequency range. Coupling to the cavity is accomplished with a loop connected to the power amplifier through a one-half wavelength transmission line. The bias power supply is included in a servo loop so that the cavity tune tracks the master oscillator. An amplitude servo is also included in the system. The cavity is shown in Fig. 6 and mechanical details of the ferrite tuning system are shown in Fig. 7.

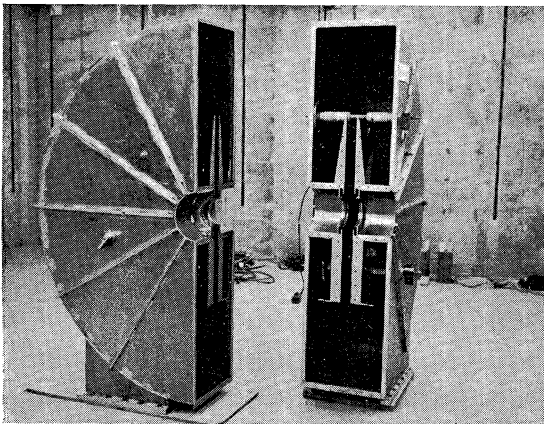


FIG. 6. Radiofrequency accelerating cavity.

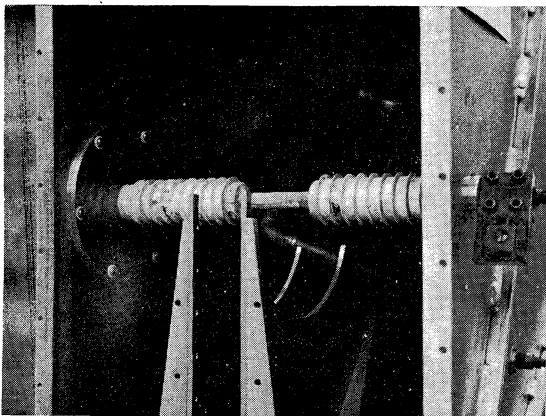


FIG. 7. Radiofrequency accelerating cavity tuning assembly. Bias current connection appears at right.

## 5. VACUUM SYSTEM

The vacuum system is constructed entirely of stainless steel and utilizes copper gaskets at flanges. Since the chamber is rather small, about 10 m in circumference, no bellows were included. The chamber sections are of  $5 \times 10$  cm elliptical cross section and were manufactured from 3 in. o.d., 0.060 in. wall tube by conventional swaging and bending techniques. Beam position monitors and clearing electrodes were included in the vacuum chamber. The curved sections were electropolished to remove the last traces of Woods metal used during the bending operations, and all sections were cleaned in Oakite before welding. A quadrant of the vacuum chamber appears in Fig. 8.

Upon completion, the vacuum chamber was assembled and given the traditional high temperature bakeout ( $350^\circ\text{C}$  for 8 hours). After cooldown, a number of small leaks were found that limited the pressure to the low  $10^{-8}$  Torr range. One of these leaks was in a vacuum pump which necessitated

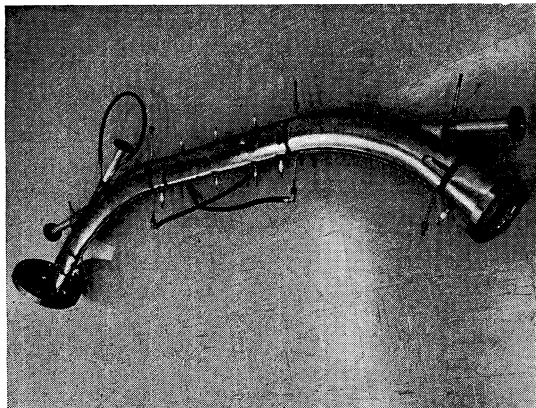


FIG. 8. Vacuum chamber octant. Two photon beam ports are shown.

letting the chamber up to atmospheric pressure for replacement of the pump. Upon reassembly, the chamber pumped down to  $2 \times 10^{-9}$  Torr in less than 24 hours without additional bakeout. The chamber was then disassembled, moved to the ring and reassembled in situ. In spite of being exposed to atmosphere for several days during this period, the chamber again pumped down to the low  $10^{-9}$  Torr range in less than 48 hours. Under continuous pumping, the chamber pressure dropped to  $8 \times 10^{-10}$  Torr by the time injection studies began two months later.

In spite of several modifications, accidents, and a number of system failures that resulted in total loss of vacuum over the past four years, the system has not been baked since the initial bakeout mentioned above. Base pressure in the system is now  $4 \times 10^{-10}$  Torr. The best pressure ever achieved was  $8 \times 10^{-11}$  Torr. This occurred during the second year of operation when, after a protracted period of operation with no failures or modifications, the tank walls had become so clean from synchrotron radiation induced outgassing that they had apparently become 'getters' themselves.

Connection between the storage ring vacuum chamber and the synchrotron radiation beam lines must, of necessity, be direct. To protect the ring,  $1\frac{1}{2}$  in. Ultek straight-through valves are installed in the beam lines so that the lines may be closed off when not in use or when experiments are being changed. These valves have been found to be compatible with the ring operating pressure, provided they are thoroughly cleaned and the elastomer

seal *lightly* lubricated with Apiezon type-L grease before installation. After installation, heating to  $150^\circ\text{C}$  drives the gas trapped in the bellows and under the elastomer out and these valves work well in the  $10^{-10}$  Torr range.

Chamber pumping is provided by five 100 liter per second sputter-ion pumps distributed about the ring as shown in Fig. 1. Initial pumping from atmospheric pressure to the  $10^{-4}$  Torr range is accomplished through the use of cryosorption pumps. Further pumping, down to the  $10^{-7}$  Torr range is carried out by pumping from the ring into the beam line separation chambers which consist of a 200 liter ion pump and a sublimation chamber. Such a unit is shown in Fig. 9. The main ring

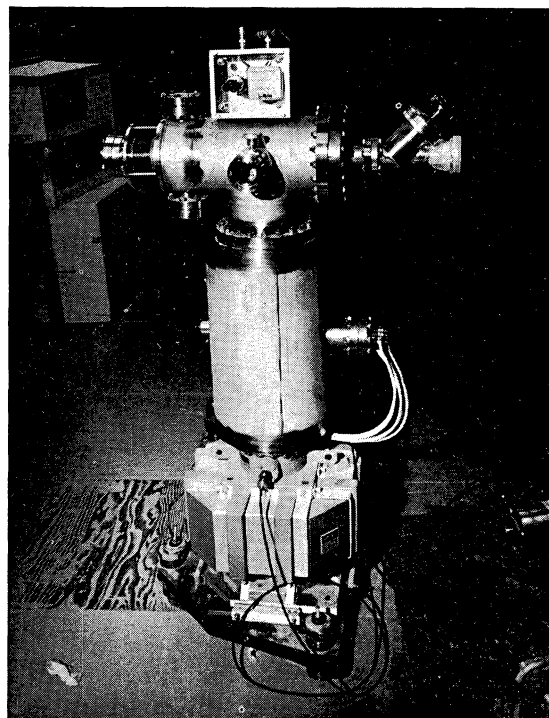


FIG. 9. Photon beam line vacuum separation chamber. Grazing incidence mirror to focus synchrotron radiation on entrance aperture of experimental system is mounted on large flange at right.

pumps are then turned on and can be relied on to bring the ring pressure down to  $2 \times 10^{-9}$  Torr in eight hours. Approximately five ampere hours of operation then brings the base pressure into the mid  $10^{-10}$  Torr range.



## 6. OPERATION

The first circulating beam was achieved in the storage ring in February of 1968. The first stored beam at full energy was achieved in March of 1968. The time interval between the first operation, i.e. stored beam at full energy, and the acquisition of the first hard data by a user was just three months. Since that time the storage ring has been operated exclusively as a synchrotron radiation source.

In spite of a heavy operations schedule (90 per cent of the funded operation time is dedicated to the synchrotron radiation research program), a number of interesting observations have been made on the storage ring during the past four years.

Measurement of the bunch length over two orders of magnitude in beam current has not shown the bunch lengthening phenomena reported by the Orsay, Frascati and Kharkov groups. The currents involved here were 0.1 to 10 mA circulating and observation was carried out with an electrostatic induction probe and sampling scope.

Early measurements of beam lifetime with small beams gave results consistent with the vacuum chamber pressure and the composition of the residual gas. However, as the beam currents achieved increased, the beam lifetime decreased. This decrease could not be explained by the pressure increase with stored beam in the ring that was a consequence of increased beam current. Neither could calculations of Touschek lifetime based on the observed beam bunch dimensions explain the short lifetime. By artificially increasing the beam cross section, initially by driving the vertical betatron motion by rf knockout techniques and subsequently by operating on a coupling resonance, we were able to determine that the beam lifetime was a function of beam current density rather than just beam current. Since this discovery, operation of the machine on the  $v_x = v_y$  coupling resonance has become standard procedure. Beam decay both on and off the resonance are shown in Fig. 10. When operating on the coupling resonance, beam lifetime is strictly a function of pressure as is shown in Fig. 11. The reasons for this phenomenon are not understood. However, it is suspected that the increased local pressure in the circulating beam due to ion trapping plays an important role.<sup>15</sup> The group at Novosibirsk has

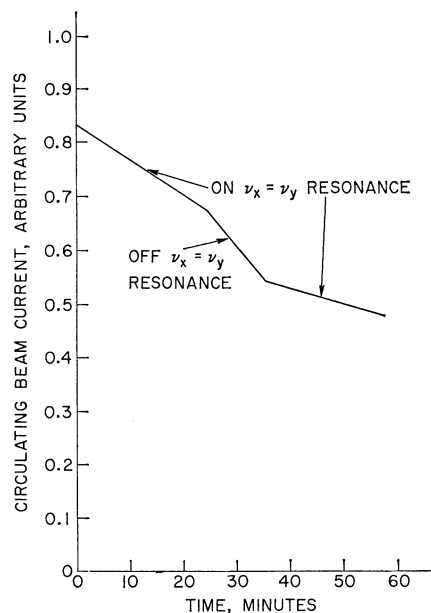


FIG. 10. Beam lifetime on and off resonance.

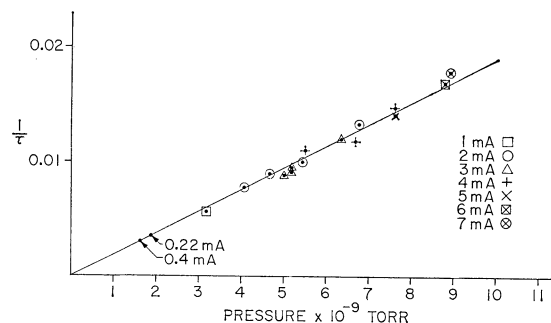


FIG. 11. Dependence of beam lifetime on beam current and vacuum chamber pressure.

noticed a similar phenomenon on VEPP-3 and they have also suggested this possibility.<sup>16</sup>

## 7. CHARACTERISTICS OF THE RADIATION

While the effects of synchrotron radiation on electron synchrotrons and storage rings are well-known to accelerator builders, it is reasonable to include a discussion of the optical and spectral properties of the radiation that make it attractive to the investigators.

Electrons traversing the magnetic field of a circular accelerator radiate energy. In their own

frame of reference, they emit in a characteristic Larmor radiation pattern, and for highly relativistic electrons, this pattern becomes strongly distorted in the forward direction as viewed by an observer in the laboratory frame. Thus, if one looks in the orbital plane, in a direction opposite to the electron's motion and tangent to the orbit, the electron will be seen as a bright point of light (single electrons circulating at 240 MeV in the storage ring can easily be seen). Even though the fundamental orbit frequency of the electrons and many higher harmonics (Fourier components) are present in the radiation, because of the distribution of synchrotron and betatron motions of the electrons a continuum spectrum is observed at the shorter wavelengths as is shown in Fig. 12. At wavelengths near the peak

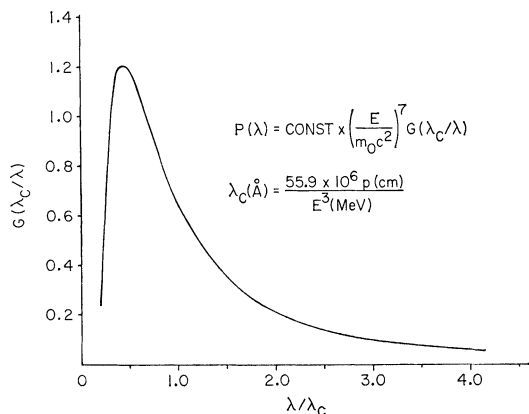


FIG. 12. Universal spectral distribution curve for the radiation from monoenergetic electrons.  $P(\lambda)$  is the instantaneous power radiated per angstrom.

of the spectrum the root mean square angle of the emission cone is given by

$$\langle \phi^2 \rangle^{1/2} \approx \gamma^{-1} \quad (1)$$

where  $\gamma = E/mc^2$ , the ratio of electron energy to rest mass energy. At 240 MeV,  $\gamma$  is 470 so the angle of the cone is about 2 mrad. Furthermore, the radiation in the plane of the orbit is polarized with electric vector oriented parallel to this plane.

Light from the electrons in orbit is unlike that from a point source, however, because of the narrow radiation cone of each electron. This natural vertical collimation of the radiation is often

overlooked when comparisons between synchrotron radiation sources and conventional X-ray tubes are made.

The power radiated per second per unit wavelength by an electron of energy  $\gamma mc^2$  with orbital radius  $R$  is given by<sup>17</sup>

$$\partial P / \partial \lambda = 3^{5/2} c e^2 \gamma^7 G(y) / 16 \pi^2 R^3 \quad (2)$$

where

$$G(y) = y^3 \int_y^\infty K_{5/3}(x) dx \quad (3)$$

The function  $G(y)$  must be evaluated numerically. However, for wavelengths such that  $y \ll 1$ ,  $G(y)$  is given approximately by<sup>18</sup>

$$G(y) \approx 2^{2/3} \Gamma(2/3) y^{7/3} \quad (4)$$

while at wavelengths such that  $y \gg 1$

$$G(y) \approx [\pi/2]^{1/2} y^{3/2} e^{-y} \quad (5)$$

Here  $c$  and  $e$  have their usual meaning and  $y = \lambda_c/\lambda$  where  $\lambda_c$  is a characteristic wavelength given by

$$\lambda_c = 4\pi R / 3\gamma^3 \quad (6)$$

The spectral function  $G(y)$  peaks at a wavelength  $\lambda_p = 0.42\lambda_c$ , reaching a value of  $\approx 1.2$ . Instead of the power emitted, spectroscopists are more interested in the total photon flux per unit wavelength. This is given by

$$dI/d\lambda = (dP/d\lambda) N \lambda / hc \quad (7)$$

where  $N = 2\pi \dot{R} J / ec$ ,  $\dot{R}$  is the average radius of the orbit and  $J$  is the average beam current density.

In general, synchrotron radiation is not coherent so that the radiated intensity just increases with the number of electrons in orbit. If, however, one could reach a very high beam density so that the distance between electrons becomes comparable with the main wavelengths of emission, coherent effects would appear. This can be seen in Eq. (2) which shows that the radiated power depends upon charge squared. In the extreme case, if  $n$  electrons are close enough together to behave as a single entity of total charge  $ne$  the power should increase as  $n^2$ .

Practical formulae for the characteristics mentioned above are as follows:

$$\lambda_c(\text{\AA}) = 5.59 R(m)/[E(\text{GeV})]^3 \quad (8)$$

and

$$\begin{aligned} dI/d\lambda \text{ (photons/sec \AA mA mrad)} \\ = 7.9 \times 10^{11} G(y) J(\text{mA}) \lambda(\text{\AA}) [E(\text{GeV})]^7 / [R(m)]^2. \end{aligned} \quad (9)$$

This last expression gives the photon flux, integrated over all vertical angles, but emitted into only 1 mrad of horizontal angle.

For the 240 MeV storage ring,  $\lambda_c = 250 \text{\AA}$ . At wavelengths such that  $y \ll 1$  the flux is independent

of particle energy and given approximately by

$$\begin{aligned} dI/d\lambda \text{ (photons/sec \AA mA mrad)} \\ = 9.35 \times 10^{13} J(\text{mA}) [R(m)]^{1/3} / [\lambda(\text{\AA})]^{4/3}. \end{aligned} \quad (10)$$

Evaluation of Eqs. (9) and (10) above leads to the figures appearing in Table II. Here, the units are number of photons per second per  $\text{\AA}$  per milliampere per milliradian. Of perhaps more interest to those working in photoelectron spectroscopy is the number of photons per electron volt,  $dI/dE$ , as a function of  $\lambda$ . This is given by

$$\begin{aligned} dI/dE \text{ (photons/sec eV mA mrad)} \\ = 5.56 \times 10^7 G(y) J(\text{mA}) [E(\text{GeV})]^7 / [R(m)]^2 \lambda^3(\text{\AA}). \end{aligned} \quad (11)$$

These figures are given in the second line of the table.

TABLE II  
Photon flux as a function of  $\lambda$ .

$\lambda$	5000 $\text{\AA}$	1000 $\text{\AA}$	500 $\text{\AA}$	100 $\text{\AA}$	50 $\text{\AA}$
$dI/d\lambda$	$8.4 \times 10^8$	$5.1 \times 10^9$	$9.85 \times 10^9$	$10^{10}$	$3 \times 10^8$
$dI/dE$	$1.48 \times 10^{12}$	$3.6 \times 10^{11}$	$1.73 \times 10^{11}$	$7 \times 10^9$	$5.27 \times 10^7$

## 8. EXPERIMENTAL PROGRAM

The range of investigations being carried out at the Synchrotron Radiation Center is wide and varied. A complete description of the experimental program now in progress at the storage ring would be far beyond the scope of this article. Thus, we will limit ourselves to a description of four experiments that to us exemplify the program and illustrate the ways in which advantage is taken of the properties of the storage ring as a photon source by the users.

The University of Illinois group, under Professor F. C. Brown, has worked from the first at the study of the transmission properties of a wide variety of solids and gases in the 60–250  $\text{\AA}$  range. Using a highly modified Hilger-Watts 1 m spectrograph, they have obtained absorption-transmission spectra on such diverse materials as the alkali halides,<sup>20</sup> nickel oxide,<sup>21</sup> pure nickel, crystalline and amorphous silicon,<sup>22</sup> aluminium,<sup>23</sup> silene,<sup>24</sup> and sulfur hexafluoride.<sup>25</sup> The resolution obtained in these measurements has been remarkable: shifts in the energy levels of the chlorine core electrons of a few tenths of an eV at 100 eV in the

alkali halides KCl and NaCl due to the chemical environment of the chlorine atoms were easily observed. In Fig. 13 we show the transmission spectrum of silene ( $\text{SiH}_4$ ) obtained by the Illinois

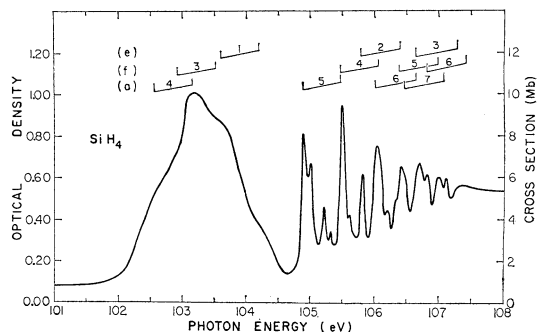


FIG. 13. Optical density of silene ( $\text{SiH}_4$ ) in the extreme ultraviolet. Courtesy of Prof. F. C. Brown, University of Illinois.

group. The structure shown pushes the resolution of the instrument, measured to be 0.025 eV at 100 eV. In addition, the Illinois group was the first at the Center to make use of the techniques of

modern particle physics in their studies, namely particle counting (in this case photons) and digital recording of data on tape for later computer analysis. These techniques are now standard at the Center and elsewhere.

Members of the Space Astronomy Laboratory of the University of Wisconsin have pursued a program aimed at the calibration of photo detectors to be flown in satellites (OAO II and others). These measurements depend on the fact that the wavelength distribution of the synchrotron radiation is exactly calculable provided that one knows the electron energy, orbit radius and the number of electrons circulating. The first two quantities can be known to high precision but the last quantity is rather difficult to measure exactly at very low circulating beam currents. The Space Astronomy group, in collaboration with the Storage Ring Operations group took the following novel approach to the problem.<sup>26</sup> Using a filter to define a segment of the spectrum and a series of absorbers calibrated for this segment of the spectral range, they were able to keep the input to their photo detectors in approximately the same intensity range as the circulating beam in the storage ring was reduced from a few thousand electrons (their calibration intensity) to approximately 100 electrons. This intensity reduction was accomplished by lowering the accelerating voltage so as to increase the loss rate due to quantum fluctuations. When approximately 100 electrons circulating was reached, changes in detector signal due to individual electrons leaving the machine were easily seen. Thus, the exact number of electrons contributing to the detector output signal was determined, assuming only detector linearity over a limited range.

As was pointed out above, synchrotron radiation is horizontally polarized. Most commercially available monochromators disperse horizontally which means that when used in their normal configurations, the polarization vector of the synchrotron radiation will be normal to the grating. While not serious for a normal incidence instrument, this 'mismatch' of polarization results in a marked decrease in the transmission efficiency of grazing incidence monochromators; as much as a factor of ten. The University of Southern California group, under Professor Darrell Judge

and Dr. Robert Carlson, designed their instrument to disperse vertically. In addition, they took advantage of the small vertical dimension of the electron beam and the natural vertical collimation of the synchrotron radiation in the shorter wavelength range by building their monochromator with no entrance slit. The resulting instrument exhibits high transmission efficiency and moderate resolution ( $\approx 0.5 \text{ \AA}$ ) and is ideal for their purposes which are to measure photo absorption, photo ionization and auto ionization cross sections in the atmospheric gases of the planets of the solar system. Through clever utilization of analog elements and by taking advantage of the extreme stability of the storage ring beam intensity with respect to time, their data acquisition system calculates and records these cross sections as the experiment proceeds.

The accurate determination of the density of electronic states in metals and other solids is a problem as old as solid state physics. These measurements have been difficult to make, not only because of the lack of sources in the 100 to 1000  $\text{\AA}$  range, but also because of the problem of surface contamination of the sample: because of the extreme absorption of radiation in this wavelength range, the photo electrons to be analyzed can only come from depths equal to those of the first few crystal planes under the surface. Even with modern high vacuum techniques, the maintenance of sample cleanliness against back-streaming gas from the monochromators and the windowless, high pressure discharge lamps commonly used for this work, is still extremely difficult. The electron storage ring which requires high vacuum for its operation and, in addition, is a continuum source, is a nearly ideal source for this work. We use the qualifier 'nearly' here because both Professor Lapeyre of Montana State University and Dr. Eastman<sup>27</sup> of IBM require some differential pumping in order to maintain  $10^{-11}$  Torr pressures in their experimental chambers against the  $10^{-9}$  operating pressure in the storage ring.

## 9. FUTURE DEVELOPMENT OF THE STORAGE RING

It was recognized from the first that the storage ring, while an intense source in 100 to 1000  $\text{\AA}$  range, would be of limited use when the investigators

turned their attention to the shorter wavelengths. For example, much interest is now being expressed in the carbon compounds. Investigation of these materials will require reasonable photon fluxes down to the carbon *K* edge (44 Å). This might be accomplished by somehow raising the energy of the storage ring to 300 MeV, thereby lowering  $\lambda_c$ , which is the approximate location of the peak of the photons per second spectrum [see Eq. (6) and Eq. (9)] to 125 Å. This, however, is not practical, and a second approach is being taken.

An array of three magnets was designed to be placed in a straight section of the storage ring (SS-3) to deflect the beam first away from and then back on to its original orbit. The central magnet of the array produces a 2.5 T field. Thus, the local radius of curvature in the central magnet will be half that

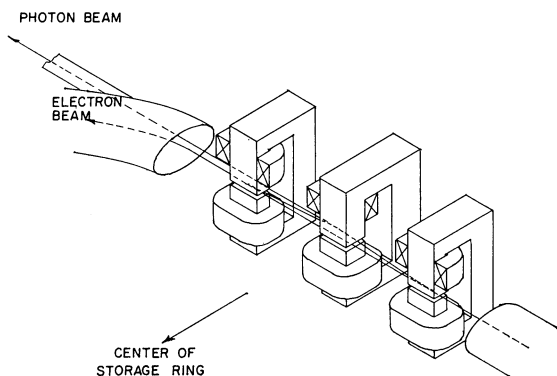


FIG. 14. Conceptual drawing of the wavelength shifter.

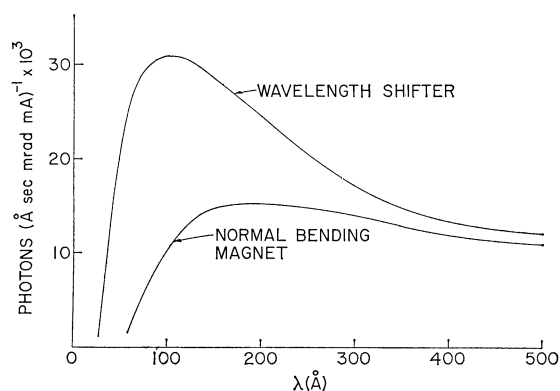


FIG. 15. Spectral characteristic of wavelength shifter photon beam compared to that of a normal bending magnet.

in a normal bending magnet and, by Eq. (8),  $\lambda_c$  will be reduced, locally, by a factor of 2. Extensive calculations have shown that the device, called the Wave Length Shifter,<sup>28</sup> will have minimal effects on the storage ring. All magnets in the device are of conventional iron-copper construction. A conceptual drawing of the ' $\lambda$  shifter' and a plot of its expected output flux in comparison to that of a normal bending magnet are given in Figs. 14 and 15. The device is now under construction and a picture of the magnet array is shown in Fig. 16.

In Section 5, mention was made of the increase in pressure in the storage ring and consequent reduction in beam lifetime due to the stored beam. Since it has been determined that beam lifetime, when operating on the  $v_x = v_y$  resonance, is strictly a function of pressure, it seemed reasonable to make an effort to improve the pressure in the storage ring under stored beam conditions. The present pumping system is conductance limited and the only way to achieve the desired improvement is to place pumps nearer to the source of gas, namely in the bending magnets. We, as others,<sup>29</sup> have developed internal pumping elements which will operate in the fringe field of the bending magnets. One such pump element, disassembled, is shown in Fig. 17. Tests on these pump elements have shown a pumping speed of greater than 250 liters per second for nitrogen and an ultimate pressure of less than  $5 \times 10^{-10}$  Torr. In agreement with the results reported by the SLAC group,<sup>30</sup> both pumping speed and ultimate pressure are essentially independent of magnetic field above 0.5 T. The operating voltage is 7 kV and the anode cell diameter is 0.500 in. There are 136 cells in the anode.

The present injector machine is now eleven years old and, because of aging of its various components, it now represents a major operational expense. Accordingly, in order to decrease operating expenses and to assure the continued high level of reliability of the storage ring complex, we have decided to replace this interesting and historic machine. Of the various machines which would be satisfactory replacements, the most attractive to us is the microtron because of its simplicity, low cost and inherently good beam quality. The microtron that is being developed at the Physical Sciences Laboratory to replace the aging FFAG synchrotron

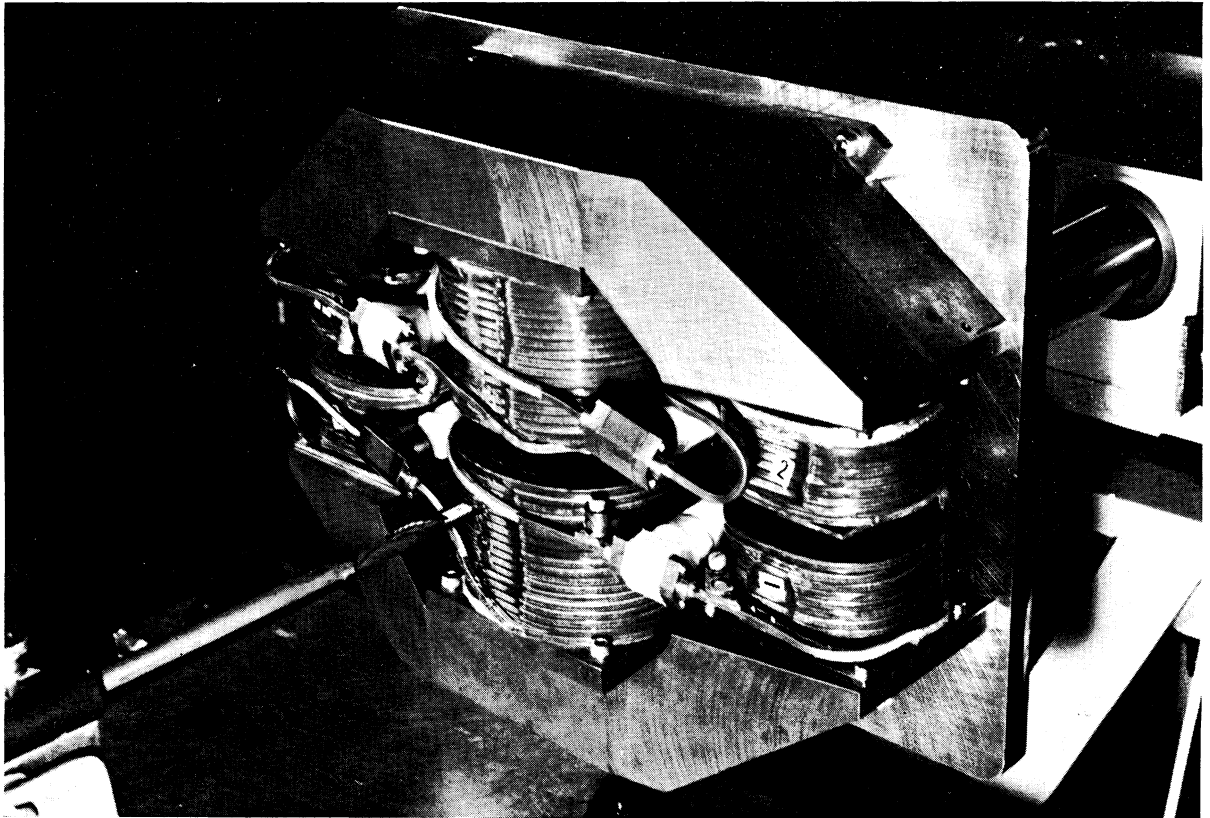


FIG. 16. Wavelength shifter magnet during magnetic field measurement.

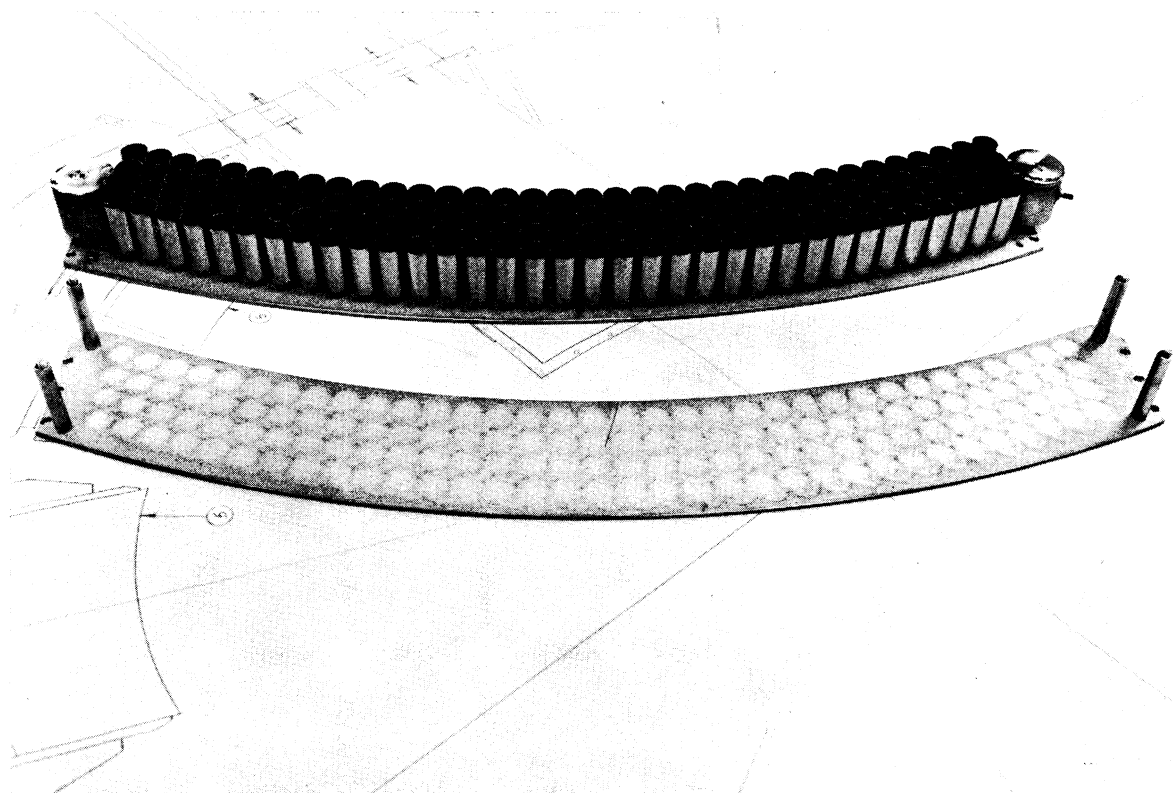


FIG. 17. Internal sputter-ion pump element.

injector is shown in Fig. 18. Several excellent reports<sup>30-32</sup> have been published in the past decade dealing with the theory and construction of the microtron. Hence, we will give only a general description of the microtron that is being built for the 240-MeV storage ring.

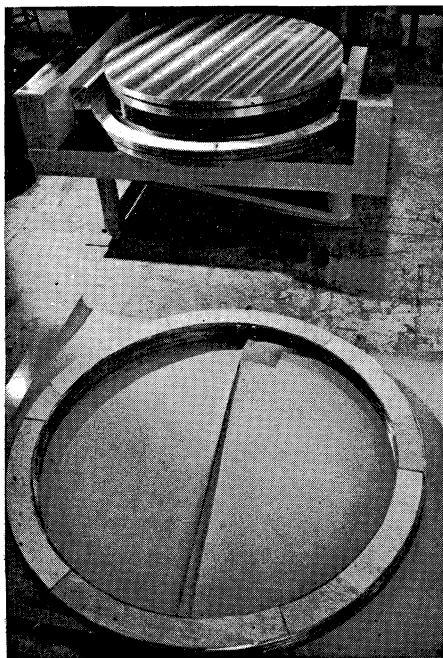


FIG. 18. 35 MeV microtron magnet. Top coil is in front of magnet.

The major operating parameters of a microtron are the energy gain per turn,  $\Delta V$ , and the mode numbers  $a$  and  $b$  defined as follows:

$$a = T_1/T_{rf} \quad (11)$$

$$b = [T_{n+1} - T_n]/T_{rf} \quad (12)$$

where  $T_{rf} = 1/\nu_{rf}$  is the period of the accelerating voltage and the integers  $n = 2, 3, 4 \dots$  correspond to the various orbits in the machine. On the  $n$ th orbit, the total energy of an electron is given by

$$E_n = m_0 c^2 + e(V_i + n\Delta V), \quad (13)$$

where  $V_i$  is the energy gain during injection. The time required for the  $n$ th orbit is evidently

$$T_n = 2E_n/Bc^2, \quad (14)$$

where  $B$  is the guide field. With a bit of rearranging we have from the above

$$\Delta V = E_0/e + V_i b/(a-b) \quad (15)$$

and

$$B = 2\pi\nu_{rf}/[c^2(a-b)][E_0/e + V_i]. \quad (16)$$

From these expressions it follows that  $a > b$ ; that the maximum value of  $B$ , the magnetic field, which gives the minimum machine diameter for a given energy is obtained with  $a-b = 1$ ; and finally that for  $a-b = 1$ , the values  $a = 2$ ,  $b = 1$  give the minimum accelerating voltage at the cavity. Two other points should be made here. The choice of the mode numbers  $a = 2$ ,  $b = 1$  also results in the largest phase acceptance<sup>30</sup> for electrons with respect to the accelerating wave and that even for  $V_i = 0$ ,  $\Delta V = 510$  kV and thus represents the lowest possible synchrotrons energy gain.

In order that the number of orbits be a minimum,  $V_i$  should be as large as possible. This is a design goal because the diameter of the machine depends directly on  $n$  through  $B$  and because the required homogeneity of the field,  $\Delta B/B$ , is proportional to  $n^{-2}$ . In practice,  $V_i$  can be made as large as  $E_0/e$  by placing the electron source on the accelerating cavity as shown in Fig. 19. Here, the injection

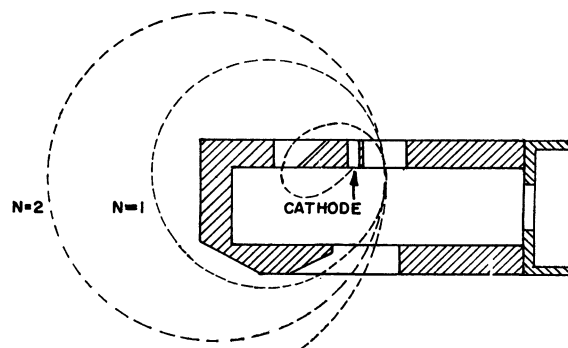


FIG. 19. Microtron accelerating cavity showing injection path and first two orbits.

orbit and orbits for  $n = 1$  and  $2$  are indicated. Other parameters that may be deduced from the above expressions, taking  $\nu_{rf}$  to be 3000 MHz, are given in Table III.

The yoke of the microtron magnet can be made of ordinary steel slabs but the pole pieces must be made of higher quality material. We, as others,<sup>32</sup> have

TABLE III  
Microtron parameters

Guide field	2000 G
$V_i$	510 kV
$\Delta V$	1020 kV
Number of orbits	34
Radius of final orbit	48 cm
Orbit spacing	3.1 cm
Magnet gap	10 cm
NI	$1.64 \times 10^4$ ampere turns

chosen to make the magnet pole pieces serve as top and bottom of the vacuum chamber. However, even if the poles were  $4\frac{1}{2}$  in. thick they would deflect approximately 0.002 in. under the air load because of their large diameter. Hence, we have modified the basic design by splitting the pole pieces in two. This may be seen in Fig. 20. The top and bottom pole pieces carry the air load while the inner pole pieces, which will be in the vacuum chamber, will have to support only their own weight. The gap between the two pole pieces also serves as a Purcell filter<sup>33</sup> or field homogenizer.<sup>34</sup>

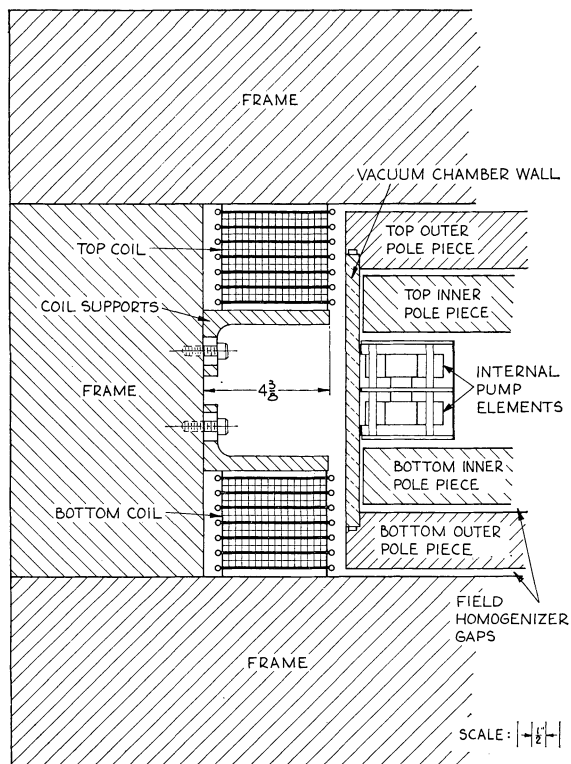


FIG. 20. Microtron cross section.

Since the vacuum system of the microtron will communicate directly with the storage ring through the beam transport line, dry pumping must be used. We will make use of internal sputter-ion pumps operating in the magnet fringe field. These will be of the same type developed for the 240 MeV storage ring.

Calculations based on the accelerating cavity geometry predict a power loss at operating voltage of 1 MW. Allowing another 500 kW for losses in the microwave system (waveguide, isolator, etc.) and electrons lost in the first few turns, we believe that beam currents of nearly 100 mA will be achievable with a 4.5 MW magnetron for a radiofrequency power source. To be conservative, we plan on 30 mA.

Since the orbits are spaced radially by 3 cm directly across from the accelerating cavity, extraction poses no difficulty. A simple iron pipe that the electrons enter at a point diametrically opposite the accelerating cavity will shield them from the weak guide field and allow them to exit from the microtron on a path tangent to the last orbit. Compensating coils will be used to prevent the presence of the iron pipe from interfering with the previous orbits.

As part of the injector replacement and vacuum chamber improvement program, we have constructed both an injector with a septum and a full aperture kicker. With these devices installed it is expected that both multiturn injection and beam stacking in the storage ring will be possible.

## 10. CONCLUSION

The research program at the 240 MeV storage ring is now four years old and, by any standard, it has been extremely successful. During this period the electron storage ring has been shown to be a nearly ideal source for vacuum ultraviolet and soft X-ray studies. Among the properties that make it so are freedom from vibration; great stability of the beam in intensity, position and energy; little if any radiation danger and compatibility with the ultrahigh vacuum requirements of many experiments. In addition, since the machine is totally dedicated to the research program, control of the source parameters, for example energy and beam position, are at the disposal of the synchrotron



radiation users. A continuous program of improvement of both the machine and the facility, is being carried out.

However, the shorter wavelengths beyond the reach of the machine promise exciting developments. Considerable interest in the 1–100 Å wavelength range is now being expressed here and abroad and preparations to use the intense X-ray continuum available from high energy electron synchrotrons for biological and electron spectroscopic chemical analysis (ESCA) studies are now being made in Germany, England, and Russia.

In view of the superiority of electron storage rings for these studies we feel that the time is not far off when an electron storage ring, with energy in the GeV range, designed specifically to be a synchrotron radiation source, will be constructed.

#### ACKNOWLEDGEMENTS

Many people participated in the construction of the storage ring and in its subsequent development. We would like to express our appreciation particularly to G. Henderson, PSL; J. W. Hicks, PSL; E. Kennedy, PSL; G. M. Lee, National Accelerator Laboratory; J. E. O'Meara, National Accelerator Laboratory; C. W. Owen, National Accelerator Laboratory; and C. H. Pruett, PSL, all of whom as members of the MURA staff during the construction period contributed greatly to the success of the machine.

During the period after construction, M. A. Green, N. C. Lien, R. A. Otte, J. D. Steben, W. S. Trzeciak, and W. R. Winter, all of the PSL staff have made significant contributions to the development of the machine and to the research program.

We would like to express special appreciation to Professor R. M. Bock, Dean of the Graduate School of the University of Wisconsin for his continued interest and support of the Synchrotron Radiation Center.

Finally, we would like to express our appreciation to the Synchrotron Radiation Users Group, particularly Professor F. C. Brown of the University of Illinois, Professor H. Fritzsche of the University of Chicago, and Professor D. Lynch of Iowa State University, for their interest, encouragement and support over the past five years.

#### REFERENCES

1. P. D. Parker, *Particle Accelerators*, **1**, 285 (1970).
2. V. F. Weisskopf, *Proc. 8th Int. Conf. on High Energy Accelerators, CERN, 1971*, p. xix.
3. D. Iwanenko and I. Pomeranchuk, *Phys. Rev.*, **65**, 343 (1944).
4. J. P. Blewett, *Phys. Rev.* **69**, 87 (1946).
5. F. R. Elder, R. V. Langmuir, and H. C. Pollock, *Phys. Rev.*, **74**, 52 (1948).
6. J. Schwinger, *Phys. Rev.*, **70**, 1912 (1949).
7. D. H. Tomboulion and P. L. Hartman, *Phys. Rev.*, **102**, 1423 (1956).
8. R. Maden and K. Codling, *J. Appl. Phys.*, **36**, 380 (1965).
9. F. C. Brown, P. L. Hartman, P. G. Kruger, B. Lax, R. A. Smith, and G. H. Vineyard, *Report of the sub-committee of the Solid State Panel of the National Academy of Sciences*, March, 1966.
10. E. M. Rowe, J. W. Hicks, and G. E. Bush, *IEEE Trans. Nucl. Sci.*, **NS-14**, No. 3, 478 (1967).
11. J. W. Hicks, *IEEE Trans. Nucl. Sci.*, **NS-14**, No. 3, 493 (1967).
12. The MURA Staff, *Proc. Int. Conf. on High Energy Accelerators, Brookhaven 1961*, p. 344.
13. F. E. Mills *et al.*, *Proc. Int. Conf. on High Energy Accelerators, Dubna 1963, USAEC Conf.-114* (1965), p. 947.
14. W. Schnell, *Proc. Int. Conf. on High Energy Accelerators, Dubna 1963, USAEC Conf.-114*, 1279 (1965), p. 405.
15. E. M. Rowe, R. A. Otte, C. H. Pruett, and J. D. Steben, *IEEE Trans. Nucl. Sci.*, **NS-16**, No. 3, 159 (1969).
16. VEPP 3 Group, *Proc. 8th Int. Conf. on High Energy Accelerators, CERN, 1971*, p. 138.
17. J. Schwinger, *Phys. Rev.*, **75**, 1912 (1949).
18. A. A. Sokolov and I. M. Ternov, *Synchrotron Radiation* (Pergamon Press, 1960), p. 30.
19. C. Gahwiller, F. C. Brown, and H. Fujita, *Rev. Sci. Instr.*, **41**, 1275 (1970).
20. See, for example, F. C. Brown, C. Gahwiller, *Phys. Rev. Letters*, **22**, 1369 (1969).
21. F. C. Brown, C. Gahwiller, and A. B. Kunz, *Sol. State Comm.*, **9**, 487 (1971).
22. F. C. Brown and O. P. Rustgi, *Phys. Rev. Letters*, **28**, 497 (1972).
23. C. Gahwiller and F. C. Brown, *Phys. Rev.*, **B2**, 1918 (1970).
24. W. Hayes, F. C. Brown, and A. B. Kunz, *Phys. Rev. Letters*, **27**, 774 (1971).
25. W. Hayes and F. C. Brown, *Phys. Rev. A*, to be published.
26. E. T. Fairchild, *Proc. Symp. on Ultraviolet and Ground Based Spectroscopy, Holland (1969)*.
27. D. Eastman, and W. Grobman, *Phys. Rev. Letters*, **28**, 1327 (1972).
28. W. S. Trzeciak, *IEEE Trans. Nucl. Sci.*, **NS-18**, No. 3, 213 (1971).
29. U. Cummings *et al.*, SLAC-Pub-797, Sept. 1970.
30. S. P. Kapitza, *The Microtron* (Science Publishing House, Moscow, 1969) (in Russian).
31. V. D. Anan'ev *et al.*, *Atomnaya Energiya*, **20**, 106 (1966).
32. V. Bizzari and A. Vignati, Frascati National Laboratory Report, LNF-69/78, December 1969.
33. E. M. Purcell, U.S. Patent 2,962,636.
34. H. A. Enge, *Nucl. Instr. and Methods*, **28**, 119 (1964).